Facile construction of hierarchical Bi@BiOBr-Bi_2MoO_6 ternary heterojunction with abundant oxygen vacancies for excellent photocatalytic nitrogen fixation

Meng Lan, Nan Zheng*, Xiaoli Dong*, Xiaolei Ren, Jiaxin Wu, Hongchao Ma, Xiufang Zhang [a]

School of Light Industry and Chemical Engineering, Dalian Polytechnic University, #1 Qinggongyuan, Dalian 116034, P R China

*Corresponding author：zhengnan@dlpu.edu.cn, dongxiaoli65@163.com

Tel: +86 411 86323009

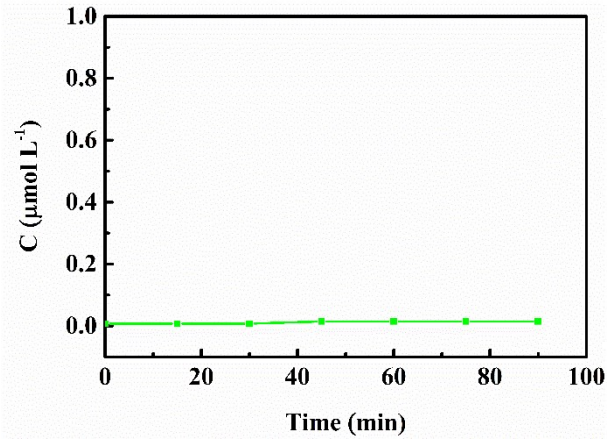

Fig. S1. The amount of N_2H_4 produced on Bi@BOB-BMO-2.

DFT calculations

The density functional theory (DFT) calculations were performed with the plane-wave techniques and implemented in the Vienna ab initio simulation package (VASP). [S1] The projector augmented wave (PAW) approach was employed to describe the ionelectron interaction. [S2] The generalized gradient approximation (GGA) in the form of the Perdew-Burke-Ernzerhof (PBE) was employed to describe the electron exchange and correlation energy. [S3] A 520 eV cutoff was adopted for all computations. DFT-D3 method with Beck-Jonson damping was adopted to accurately account for the weak interactions. [S4] A Monkhorst-Pack k-point mesh of 6×6×3 was used for BiOBr unit cell, 4×4×1 for BiOBr(001)-c(2x2), Bi_2MoO_6(001)-p(1x1) and BiOBr(001)/Bi_2MoO_6(001) heterojunction surface models. For surface models, a vacuum space with 15 A was inserted in the *z* direction to prevent the artificial interaction between periodically repeated images. The adsorption energy (Eads) of N_2 molecules was defined as $Eads = E_{tot} - E_{slab} - E_{N2}$, in which E_{tot}, E_{slab} and E_{N2} stand for the total energy of the complex of the catalysts and N_2, the catalysts and isolated N_2 molecule, respectively.

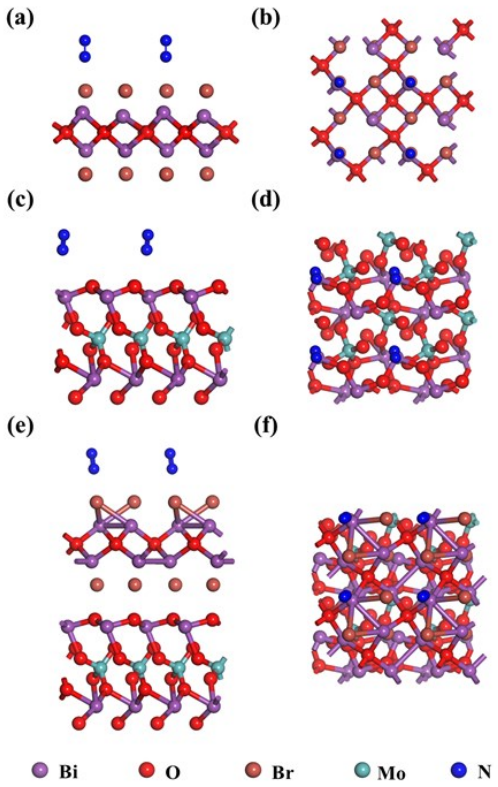

Fig. S2. Schematic illustration of optimized adsorption geometries of N_2 on the (001) surface of (a,b) BOB with OVs, (c,d) BMO and (e,f) Bi@BOB-BMO ((a,c,e) side and (b,d,f) top views).

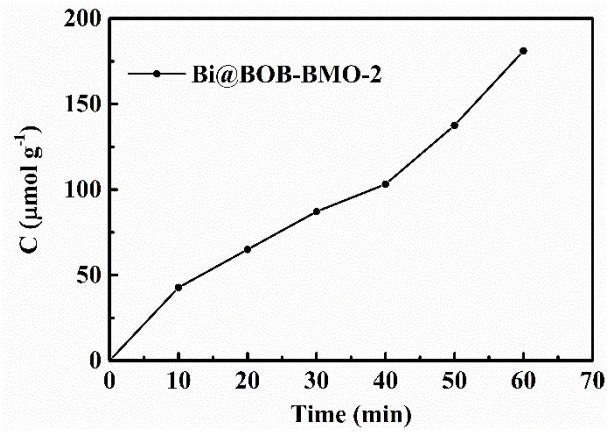

Fig. S3. O_2 generation along with photocatalytic nitrogen fixation of Bi@BOB-BMO-2.

Table S1. Photocatalytic nitrogen fixation over different photocatalysts under various reaction conditions.

Photocatalyst	Scavenger	Light source	Ammonia detection method	NH_3 rate	Ref.
Single-Unit-Cell Bi_3O_4Br Nanosheets	No	300 W Xe lamp full spectrum	ion exchange chromatography	48.3 μmol g^{-1} h^{-1}	[S5]
Ultrathin TiO_2 nanosheets	No	300 W Xe lamp 200-800 nm	ion exchange chromatography	78.9 μmol g^{-1} h^{-1}	[S6]
$W_{18}O_{49}$ by Mo doping	Na_2SO_3	300W Xe lamp full spectrum	ion exchange chromatography	176.2 μmol g^{-1} h^{-1}	[S7]
$Ru/RuO_2/g\text{-}C_3N_4$	Methanol	300W Xe lamp full spectrum	ion exchange chromatography	13.3 μmol g^{-1} h^{-1}	[S8]
Ultrathin BiOBr nanosheets	No	300 W Xe lamp, full spectrum	Nessler's reagent	54.70 μmol g^{-1} h^{-1}	[S9]
BiOBr with oxygen vacancies	No	300 W Xe lamp, λ >420 nm	Nessler's reagent	104.2 μmol g^{-1} h^{-1}	[S10]
Fe doped BiOBr nanosheets	No	300 W Xe lamp with a 420 nm cutoff filter	Nessler's reagent	382.68 μmol g^{-1} h^{-1}	[S11]
Bi deposited $InVO_4$ nanosheets	No	300 W Xe lamp, full spectrum	Nessler's reagent	626 μmol g^{-1} h^{-1}	[S12]
Fe-mediated Bi_2MoO_6	No	300 W Xe lamp, λ >400 nm	Nessler's reagent	106.5 μmol g^{-1} h^{-1}	[S13]
Bi_2MoO_6/BiOBr heterojunctions	No	300 W Xe lamp, full spectrum	Nessler's reagent	81.0 μmol g^{-1} h^{-1}	[S14]
Bi@BiOBr-Bi_2MoO_6 heterojunction	No	300 W Xe lamp, full spectrum	ion exchange chromatography	167.15 μmol g^{-1} h^{-1}	This work

Table S1 displays the photocatalytic nitrogen fixation performance of our Bi@BiOBr-Bi_2MoO_6 ternary heterojunction relative to other similar photocatalysts under various reaction conditions. As shown in columns 5 of Table S1, among the numerous bismuth photocatalysts, the nitrogen fixation level of our photocatalyst fall within the mid-range of all other photocatalysts.

References

S1. G. Kresse, J. Furthmu¨ller, *Phys. Rev. B*, 1996, **54**, 11169–11186.

S2. G. Kresse, D. Joubert, *Phys. Rev. B*, 1999, **59**, 1758–1775.

S3. J. Perdew, K. Burke, M. Ernzerhof, *Phys. Rev. Lett.*, 1996, **77**, 3865-3868.

S4. S. Grimme, S. Ehrlich, L. Goerigk, *J. Chem. Phys.*, 2011, **32**, 1456–1465.

S5. J. Di, J. Xia, M. F. Chisholm, J. Zhong, C. Chen, X. Cao, F. Dong, Z. Chi, H. Chen, Y. X. Weng, J. Xiong, S. Z. Yang, H. Li, Z. Liu and S. Dai, *Adv. Mater.*, 2019, **31**, 1807576-1807583.

S6. Y. Zhao, Y. Zhao, R. Shi, B. Wang, G. I. N. Waterhouse, L. Z. Wu, C. H. Tung and T. Zhang, *Adv. Mater.*, 2019, **31**, 1806482-1806490.

S7. N. Zhang, A. Jalil, D. Wu, S. Chen, Y. Liu, C. Gao, W. Ye, Z. Qi, H. Ju, C. Wang, X. Wu, L. Song, J. Zhu and Y. Xiong, *J. Am. Chem. Soc.*, 2018, **140**, 9434-9443.

S8. H. Wang, X. Li, Q. Ruan and J. Tang, *Nanoscale*, 2020, **12**, 12329-12335.

S9. X. Xue, R. Chen, H. Chen, Y. Hu, Q. Ding, Z. Liu, L. Ma, G. Zhu, W. Zhang, Q. Yu, J. Liu, J. Ma and Z. Jin, *Nano. Lett.*, 2018, **18**, 7372-7377.

S10. H. Li, J. Shang, Z. Ai and L. Zhang, *J. Am. Chem. Soc.*, 2015, **137**, 6393-6399.

S11. Y. Liu, Z. Hu and J. C. Yu, *Chem. Mater.*, 2020, **32**, 1488-1494.

S12. J. Wang, C. Hua, X. Dong, Y. Wang and N. Zheng, *Sustain. Energy Fuels*, 2020, **4**, 1855-1862.

S13. Q. Meng, C. Lv, J. Sun, W. Hong, W. Xing, L. Qiang, G. Chen and X. Jin, *Appl. Catal., B*, 2019, **256**, 117781.

S14. X. Xue, R. Chen, C. Yan, Y. Hu, W. Zhang, S. Yang, L. Ma, G. Zhu and Z. Jin, *Nanoscale*, 2019, **11**, 10439-10445.